Provided for non-commercial research and education use.
Not for reproduction, distribution or commercial use.

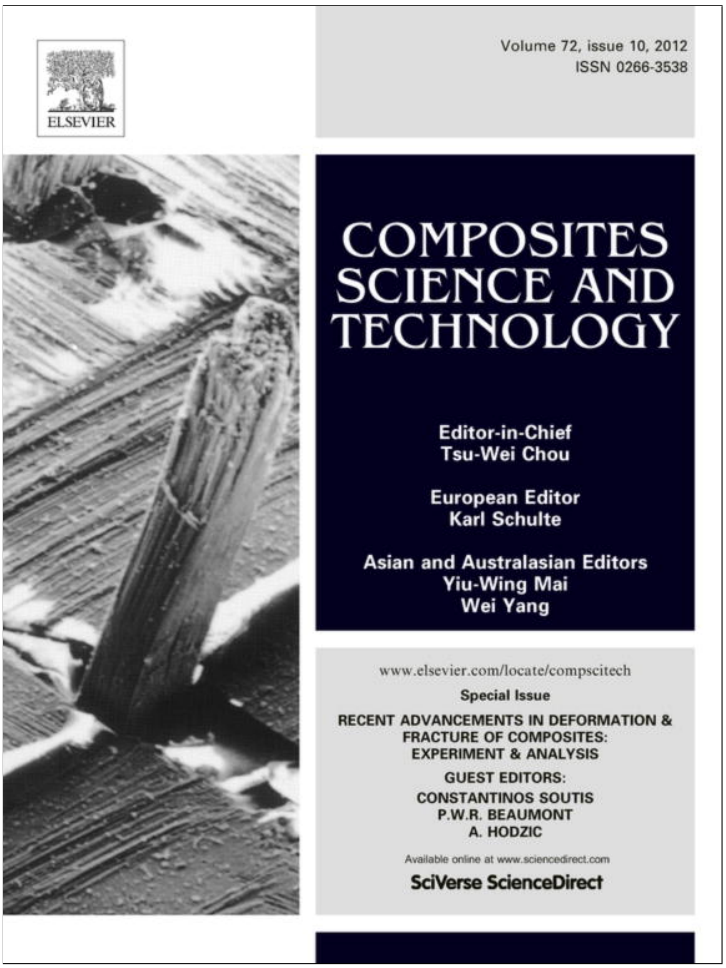


This article appeared in a journal published by Elsevier. The attached copy is furnished to the author for internal non-commercial research and education use, including for instruction at the authors institution and sharing with colleagues.

Other uses, including reproduction and distribution, or selling or licensing copies, or posting to personal, institutional or third party websites are prohibited.

In most cases authors are permitted to post their version of the article (e.g. in Word or Tex form) to their personal website or institutional repository. Authors requiring further information regarding Elsevier's archiving and manuscript policies are encouraged to visit:

http://www.elsevier.com/copyright

Author's personal copy

Composites Science and Technology 72 (2012) 1147–1152

Contents lists available at SciVerse ScienceDirect

Composites Science and Technology

journal homepage: www.elsevier.com/locate/compscitech

# Conditions of applying Oliver–Pharr method to the nanoindentation of particles in composites

Wenyi Yan [a,*], Chung Lun Pun [a], George P. Simon [b]

[a] Department of Mechanical & Aerospace Engineering, Monash University, Clayton VIC 3800, Australia
[b] Department of Materials Engineering, Monash University, Clayton VIC 3800, Australia

ARTICLE INFO

*Article history:*
Received 24 June 2011
Received in revised form 18 January 2012
Accepted 21 March 2012
Available online 29 March 2012

*Keywords:*
A. Particle-reinforced composites
C. Elastic properties
C. Finite element analysis
Nanoindentation

ABSTRACT

The indentation test is a popular experimental method to measure a material's mechanical properties such as elastic modulus and hardness, and the Oliver–Pharr method is commonly used in commercial indentation instruments to obtain these two quantities. To apply the Oliver–Pharr method correctly in all of these cases, it is essential to know the limitations of this method. The present study focuses on the applicability of the Oliver–Pharr method to measure the mechanical properties of particles in composites. The finite element method is used to undertake virtual indentation tests on a particle embedded in a matrix. In our numerical studies, the indentation "pile-up" phenomenon is generally observed in our numerical case studies, which indicates that the contact area used for predicting the elastic modulus should be measured directly, not be estimated from the indentation curve. The Oliver–Pharr method based on the real contact area is applied to estimate the elastic modulus of the particles by using the indentation curve from the numerical simulation, with the estimated elastic modulus being compared with the input value. Applying the real contact area value (not the one predicted from the indentation curve) we show that the Oliver–Pharr method can still be applied to measure the elastic modulus of the particle with sufficient accuracy if the indentation depth is smaller than the particle-dominated depth, a value defined in this work. The influences of the matrix and particle properties on the particle-dominated depth are studied using a dimensional analysis and parametric study. Our results provide guidelines to allow the practical application of the Oliver–Pharr method to measure the elastic modulus of particles in composites. This could be particularly important where particles are formed *in situ* in a matrix (as opposed to being preformed and subsequently incorporated in a matrix), or when the modulus of individual performed particles is required such as for subsequent modelling, but the modulus of individual material particles (or its material) cannot readily be determined.

© 2012 Elsevier Ltd. All rights reserved.

## 1. Introduction

In an instrumented indentation (nanoindentation) test, a hard indenter is pressed into the surface of a specimen to depths ranging from nanometers to micrometers, and the curve of the indentation force versus the indentation depth is recorded. The measured indentation curve is a function of the mechanical properties of the tested specimen. Therefore, if an inverse analysis method can be found, the mechanical properties of the tested specimen can be predicted from the measured indentation curve. Due to its simplicity, convenience and the increasing availability of commercial nanoindentation instruments, such as Hysitron Triolab™ and MTS Nano Indenter® system, the nanoindentation test has become a widely-used experimental method to probe the mechanical properties of different materials [1–7].

With regards to its application of characterizing particle-reinforced composites or more generally, inhomogeneous materials, Leggoe [8] developed an approximation method to predict the elastic modulus of the particle based on FEA simulations of a stiff particle embedded in a soft matrix and a theoretical analysis for spherical indentation under a multiple partial-unloading indentation regime. This method was subsequently used to measure the elastic moduli of silicon carbide particles and Micral™ microspheres in two aluminum-matrix particulate reinforced metal matrix composite. Nanoindentation has also been applied to measure the elastic modulus and hardness of dendrite particles dispersed in a Zr-based bulk metallic glass composite for the purpose to study the contribution of the dendrite particles on the ductility improvement of the glassy alloy [9]. Pradhan et al. [10] reported a nanoindentation test of the elastic modulus and hardness of graphite flakes and spherulites embedded in spheroidal graphite iron. The particle inclusions are important to the strength and ductility of the cast iron. Delincé et al. [11] carried out nanoindentation tests

* Corresponding author. Tel.: +613 99020113; fax: +613 99051825.
*E-mail address:* wenyi.yan@monash.edu (W. Yan).

0266-3538/$ - see front matter © 2012 Elsevier Ltd. All rights reserved.
http://dx.doi.org/10.1016/j.compscitech.2012.03.019

Author's personal copy



on individual ferrite and martensite phases in a fine-grained dual phase steels for purpose to separate the strengthening contributions of the two phases to the dual phase steels.

The theory for using instrumented nanoindentation to probe the elastic modulus of materials was developed by Oliver and Pharr in 1992 [12]. However, the Oliver–Pharr method is only suitable for monolithic and isotropic materials. When it is applied to particles in composites, the measured elastic modulus is a function of the elastic properties of both the particle and the matrix. In particular, the influence of the matrix on the measured elastic modulus for the particles should be understood in order to understand and use the measured data. Additionally, the method described by Oliver–Pharr to predict the projected contact area under load (a prerequisite step to determine the elastic modulus and hardness) is only suitable for the indentations which display the deformation phenomenon of "sink-in", where the surface around the indenter sinks in, see Fig. 1a. If the opposite indentation deformation phenomenon of "pile-up" occurs (the surface of the sample around the indenter being at a greater level than its surrounds, see Fig. 1b), the predicted contact area is smaller than the real one. Therefore, the elastic modulus and hardness can be significantly overestimated [13] (see next section).

In our recent research on the indentation of a particle embedded in a matrix [14], two cases were studied, that of a stiff particle embedded in a soft matrix and a soft particle embedded in a stiff matrix. It was found that complicated, pile-up deformation occurred in both of these representative cases from our numerical simulations, and thus that the indentation force versus depth curve cannot be applied to accurately estimate the real contact area under load. The more important fundamental conclusion was that there exists a particle-dominated depth in both cases, and that if the indentation depth is within this particle-dominated depth, the Oliver–Pharr method can still be applied to measure the particle's elastic modulus with sufficient accuracy, provided that the real contact area under load is used in the prediction. In this paper, dimensional analysis and the finite element simulations were carried out to further examine the influence of the material properties on the particle-dominated depth. The results from this work provide guidelines for measuring the elastic modulus of a particle embedded in a matrix, or more generally, measuring the elastic modulus of an inclusion/defect in an inhomogeneous material.

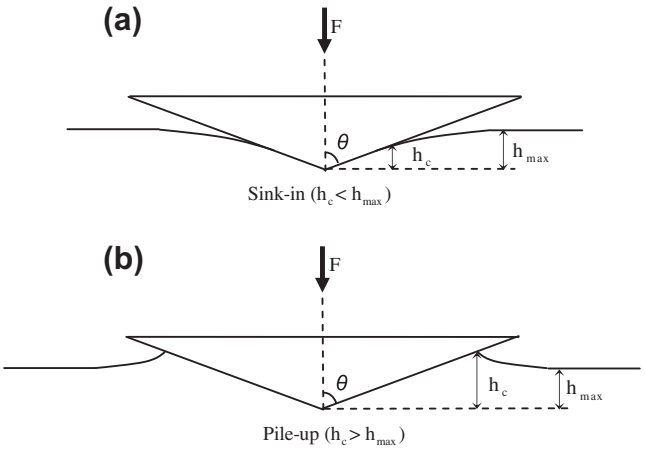


**Fig. 1.** Schematics of sink-in (a) and pile-up (b).

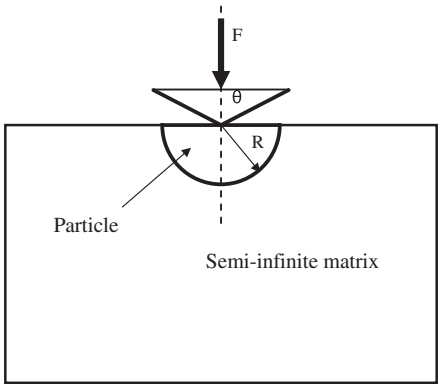


**Fig. 2.** Schematic illustration of the theoretical indentation model.

## 2. Investigation model and method

### 2.1. Theoretical model

Particle reinforced composites, or inclusions in inhomogeneous materials, are considered in this research. An idealized semi-spherical particle embedded in the surface of a semi-infinite matrix is investigated in this work, as shown in Fig. 2. This model corresponds to a real situation of particles discretely distributed in a matrix with a relatively low particle volume fraction. A conical indenter with 70.3° was pressed at the center of the semi-spherical particle. This conical indenter is equivalent to a sharp Vickers or Berkovich indenter [15], which is commonly used in commercial indentation instruments.

The illustrated indentation in Fig. 2 was simulated in a virtual fashion by using an axisymmetric finite element model, see Fig. 3. The commercial finite element package Abaqus was utilized for the simulations. To ensure the accuracy of the numerical results, contact between the specimen and the indenter tip always occurs at a very fine mesh zone. Several finite element models were utilized for different cases. A typical FE model contains a total of 21,012 eight-noded quadratic axisymmetric elements. Loading increment was also controlled to ensure smooth indentation curves. A typical indentation loading and unloading simulation took about 2.5 h with 2CPUs on an Oracle/Sun Constellation Cluster supercomputer at National Computational Infrastructure in Canberra, Australia.

The specimen size and the mesh density near the contact zone were first determined according to Sneddon's theory for an elastic indentation with a sharp indenter [16]. An elastic indentation with a single phase material was simulated and the predicted indentation curve was compared with Sneddon's theory until a satisfied result with the error no large than 5% was obtained. Additionally, the mesh to be used for the study was checked to ensure a convergent result (here the particle-dominated indentation depth, see Section 2.3) is achieved, i.e, further refining the mesh will not affect the result.

After finalizing the finite element models, indentation simulations were carried out. The output indentation force versus the indentation depth curve was then used to predict the elastic modulus of the particle by strictly following the Oliver–Pharr method, which duplicates the procedure conducted by a nanoindentation instrument in a real, physical test. For this purpose, the Oliver–Pharr method was first briefly discussed below.

### 2.2. Oliver–Pharr method

The Oliver–Pharr method is the most common method for establishing the projected contact area and predicting the elastic modulus of ordinary materials. This method begins by fitting the

Author's personal copy



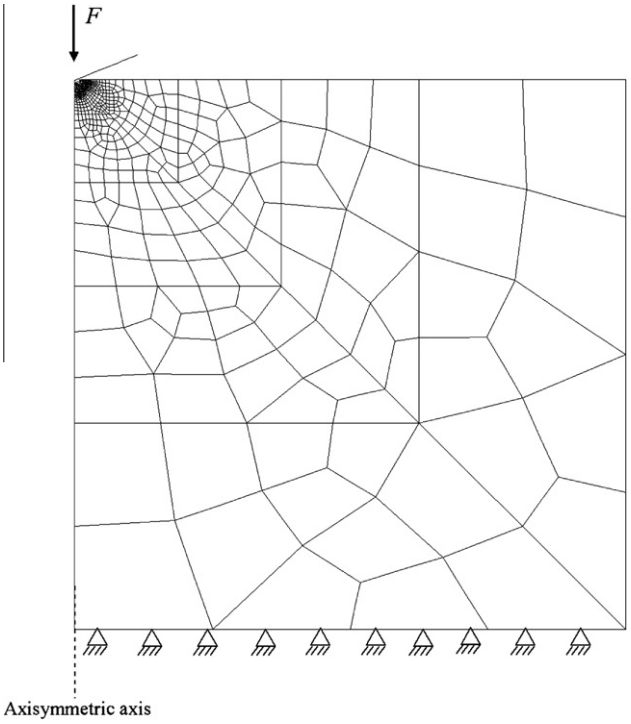


**Fig. 3.** Axisymmetric finite element model to simulate the indentation test with a rigid conical indenter.

unloading portion of the indentation graph data to the power-law relation as below [12,17],

$$F = B(h - h_f)^m \tag{1}$$

where $B$ and $m$ are fitting parameters and $h_f$ is the final indentation depth after complete unloading. From this data the initial unloading slope, i.e., contact stiffness, $S$, can be estimated by analytically differentiating Eq. (1) and evaluating the result at the maximum indentation depth, i.e.,

$$S = \left(\frac{dF}{dh}\right)_{h=h_{\max}} = Bm(h_{\max} - h_f)^{m-1} \tag{2}$$

The obtained contact stiffness from Eq. (2) is then used to estimate the contact depth $h_c$ under the maximum indentation force,

$$h_c = h_{\max} - \varepsilon\frac{F_{\max}}{S} \tag{3}$$

where $\varepsilon$ is a constant which depends on the indenter geometry. For conical indenters, $\varepsilon$ has been suggested to be 0.72 [15]. The projected contact area, $A$, under the maximum indentation force for a sharp conical indenter is determined by the indenter tip's included angle, $\theta$, and the estimated contact depth, $h_c$, from Eq. (3), that is,

$$A = \pi(h_c \tan\theta)^2 \tag{4}$$

Finally, in the case of a rigid indenter, as assumed here, the elastic modulus of the particle, $E_p^m$, can be calculated by

$$E_p^m = \frac{1}{\beta}\frac{\sqrt{\pi}}{2}\frac{S}{\sqrt{A}}(1 - \nu_p^2) \tag{5}$$

where $\nu_p$ is the Poisson's ratio of the particle and $\beta$ is a correction factor. A value of 1.05 for $\beta$ was recommend by Oliver and Pharr [17] and used in this investigation.

Applying Eqs. (3) and (4) to estimate the projected contact area is strictly based on the indentation phenomenon of sink-in, where the surface around the indenter is lower than the sample as a whole, as illustrated in Fig. 1a. Our case studies show that a complicated pile-up deformation would occur in the indentation of a particle embedded in a matrix [14], see Fig. 4. Therefore, instead of applying Eqs. (3) and (4), the projected contact area is obtained directly from our FE simulation in the current investigation. In a true practical experimental sense, the real contact area under the maximum indentation force for a sharp conical indenter can readily be obtained from imaging techniques, such as SEM and AFM. It is worth mentioning that a very large indentation depth (force) was applied in the case studies shown in Fig. 4, for the purpose of amplifying the complicated pile-up deformation around the indenter tip and between the particle and the matrix. The deformation due to the large force would cause interfacial failure between the particle and the matrix, see Fig. 4a. However, when instrumented nanoindentation is used to measure elastic modulus in practice, the indentation depth is much smaller and will not cause such interfacial failure. Therefore, there is no need to consider the interfacial debonding in our numerical modelling.

### 2.3. Particle-dominated indentation depth

It is understandable that the matrix would affect the measured elastic modulus of the particle from an indentation test. The influence of the matrix depends on the relative indentation depth with respect to the particle radius. If the indentation depth normalized by the particle radius is too large, the measured elastic modulus will be significantly different from the real value of the particle's

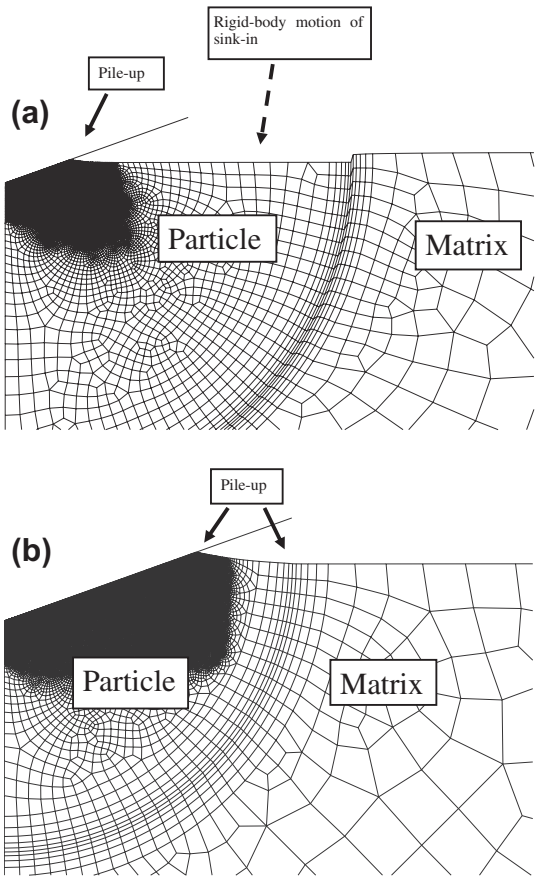


**Fig. 4.** Deformed particle and the surrounding matrix at the indentation depth of $h_{\max}/R = 0.25$ for (a) a stiff particle embedded in a soft matrix, which shows local pile-up around the indenter and large rigid-body motion of sink-in of the particle; (b) a soft particle embedded in a stiff matrix, which shows double pile-up of the soft particle material around the indenter and around the interface between the particle and the matrix [14].

Author's personal copy



elastic modulus. On the other hand, if the normalized indentation depth is small enough, the influence of the matrix can be neglected and the measured elastic modulus can be accepted as the elastic modulus of the particle. Based on this rationale, the concept of particle-dominated indentation depth is introduced to exclude the influence of the matrix on the measured elastic modulus. The particle-dominated indentation depth is the threshold indentation depth normalized by the particle radius. If the normalized indentation depth is smaller than the particle-dominated indentation depth, the measured elastic modulus is theoretically within 10% of the elastic modulus of the particle. Put differently, the error to measure the elastic modulus of the particle will be no larger than 10% if the indentation depth is smaller than the particle-dominated indentation depth in a practical indentation test. In this study, the error tolerance is chosen as 10%, which is considered to be practically acceptable. For a given particulate composite and a given tolerance, the value of the particle-dominated depth is determined. The detailed procedure to determine the particle-dominated depth for a given particulate composite is described below.

Firstly, a set of virtual indentation tests with different indentation depths are carried out using the finite element method, which is described in Section 2.1. Secondly, the unloading curves and the projected contact areas at different indentation depths are recorded, and they are used to predict the elastic modulus of the particle by following the Oliver–Pharr method. Thirdly, the predicted elastic moduli ($E_p^m$) at different depths are normalized by the real value of the particle's modulus ($E_p$) (the input value in the FE simulations), and the curve of the normalized modulus ($E_p^m/E_p$) versus the normalized indentation depth ($h_m/R$) can be plotted. To demonstrate the procedure, the $E_p^m/E_p$ versus ($h_m/R$) curves from two case studies are illustrated in Fig. 5. Case One corresponds to a composite system with the elastic modulus of the particle smaller than that of the matrix, $E_p < E_m$. As expected, the predicted particle modulus in this case increases with the indentation depth, the curve with square marks in Fig. 5, which indicates that the influence of the matrix increases with the depth. Case Two is for a composite system with $E_m < E_p$. It can be seen that the predicted particle modulus decreases with the indentation depth due to the increasing influence of the matrix, the curve with diamond marks in Fig. 5. The final step is to locate the intersection point between the normalized modulus curve and the error tolerance curve ($E_p^m/E_p = 1.1$ or $E_p^m/E_p = 0.9$). The abscissa of the intersection point is the required particle-dominated depth for the given particulate composite. Here, the particle-dominated indentation depths are 0.138 and 0.097, respectively, for Case One and Case Two. Practically, this means that the accuracy of the measured elastic modulus of the particle will be over 90% if the indentation depth is smaller than 13.8% of the particle radius for Case One and 9.7% of the radius for Case Two. To apply the particle-dominated depth as a guideline to measure the elastic modulus of a particle embedded in a matrix in practice, it is important to understand the effects of the other parameters on the particle-dominated depth, which is examined by the dimensional analysis and parametric study in the following section.

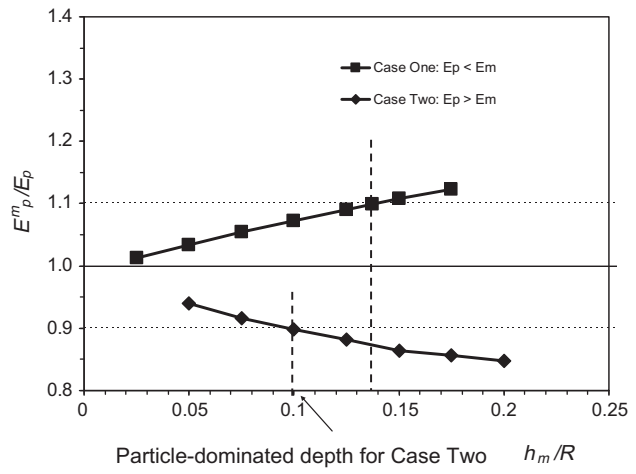


**Fig. 5.** Illustration of the method to determine the particle-dominated depth normalized by the particle radius for two cases: Case One with $E_p < E_m$ and Case Two with $E_p > E_m$.

## 3. Parametric study of particle-dominated indentation depth

### 3.1. Dimensional analysis

The particle-dominated indentation depth has different values for different material systems. To find the conditions to cover a range of material systems, dimensional analysis and parametrical study are carried out. Dimensional analysis is a powerful tool to systematically examine a research problem and it has been successfully applied to study nanoindentation mechanics. For example, for conical indenters, Cheng and Cheng [18] used the established scaling relationships from dimensional analysis to demonstrate that the indentation force is proportional to the square of the indenter displacement and that the hardness is independent of the indenter displacement. Based on dimensional analysis and numerical results, we proposed a method to use spherical indentation test to measure the plastic properties of metallic foams [6].

According to our understanding of the physical problem, for a given composite system, the absolute value of the particle-dominated indentation depth ($h_p$), i.e., before normalized by the particle radius, depends on the material properties of the particle and the matrix, the geometry of the particle and the indenter, but independent of the maximum indentation force or depth. Therefore, we have,

$$h_p = f(E_p, \upsilon_p, Y_p, n_p, E_m, \upsilon_m, Y_m, n_m, \theta, R) \tag{6}$$

where $\upsilon_p$ and $\upsilon_m$ are the Poisson's ratios of the particle and the matrix, respectively. $Y_p$ and $n_p$ are the plastic yield strength and plastic hardening index for the particle and $Y_m$ and $n_m$ are the two corresponding parameters for the matrix. $\theta$ is the included angle of the sharp indenter, see Fig. 2. Practically, the commonly used sharp indenters are three-sided pyramid Berkovich indenter and four-sided pyramid Vickers. From the modelling point of view, a conical indenter with the included angle of 70.3°, which is used in our current investigation, is equivalent to a real Berkovich or Vickers indenter as it provides the same projected contact area for the same depth [15]. In most of the cases, the indentation depth for measuring the elastic modulus of the particle is too small to cause plastic deformation of the matrix. Therefore, the parameters $Y_m$ and $n_m$ to describe the plasticity of the matrix can be removed from Eq. (6) to simplify our analysis. It should be noted that the plastic deformation could occur in the extreme cases of a very stiff particle and a matrix with very low yield strength. Such cases can be considered in the future. With regard to the plasticity of the particle, the hardening behavior is neglected, i.e., $n_p = 0$. The plastic hardening has negligible influence on the modulus prediction from an indentation test of a single phase material. It is expected that it will not affect the particle-dominated indentation depth significantly. Additionally, the values of the Poisson's ratio for both of the particle and the matrix are taken as a constant 0.3 in our following investigation, however any variation from this will lead to only a very limited change in the measured indentation modulus, see Eq. (5). Therefore, it is believed that the variation of the Poisson's ratios from 0.3 will not

Author's personal copy



affect the particle-dominated depth significantly. Based on all these considerations, Eq. (6) can be simplified as

$$h_p = f(E_p, Y_p, E_m, R) \tag{7}$$

According to Buckingham Π theorem for dimensional analysis, we choose $E_m$ and $R$ as the primary quantities in our problem with two fundamental dimensions, length and force. The dimensionless scaling relationship for the particle-dominated indentation depth is

$$\frac{h_p}{R} = \prod\left(\frac{E_p}{E_m}, \frac{Y_p}{E_m}\right) \tag{8}$$

### 3.2. Numerical results

Applying the numerical model described in Section 2.1, finite element simulations were carried out to illustrate the scaling relationship Eq (8). Because the results for the composite systems of a soft particle and a stiff matrix ($E_p/E_m < 1$) are quite different for those of a stiff particle and a soft matrix $E_p/E_m > 1$, the two types of composite system are discussed separately.

Fig. 6 shows the particle-dominated indentation depth, $h_p/R$, as a function of the elastic modulus ratio between the particle and the matrix, $E_p/E_m$ with different values of the normalized particle's yield strength, $Y_p/E_m$ for the composite systems of a soft particle and a stiff matrix, i.e., $E_p/E_m < 1$. For a given value of $Y_p/E_m$, the numerical results show that the particle-dominated depth increases with the elastic modulus ratio $E_p/E_m$, especially in the region of $E_p/E_m > 0.5$. When the elastic modulus of the particle approaches that of the matrix, i.e., $E_p/E_m$ tends towards one, and the composite trends towards a single phase material. For a single phase material, the particle-dominated indentation depth is theoretically infinite. This is shown by Fig. 6 where the particle-dominated indentation depth can be seen to increase rapidly when $E_p/E_m > 0.5$. Considering the error tolerance is 10% (Fig. 5), it is difficult to obtain a numerical result of $h_p/R$ when $E_p/E_m$ approaches one and thus the numerical curves stop at $E_p/E_m = 0.75$ or $E_p/E_m = 0.8$.

Fig. 6 shows that the particle's yield strength will also affect the particle-dominated indentation depth for the type of composite systems with a soft particle and a stiff matrix. $h_p/R$ increases with the increase of $Y_p/E_m$. The values of $Y_p/E_m$ considered here from 0.003 to 0.05 have covered a wide range of materials. In terms of the potential application of results in Fig. 6 in guiding the indentation method to measure the elastic modulus of the particle, firstly $E_p/E_m < 1$ can be determined from the measured modulus versus indentation depth curve. Referring to Fig. 5, if the measured modulus increases with the indentation depth, then it indicates that $E_p/E_m < 1$ and Fig. 6 can be applied. Considering the value of the particle's yield strength is unknown, a reasonable value of $h_p/R = 5\%$ can be recommended from Fig. 6.

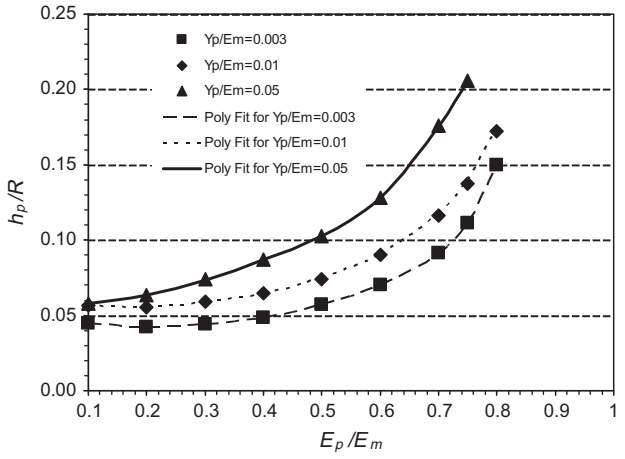


**Fig. 6.** The particle-dominated indentation depth, $h_p/R$, as a function of the elastic modulus ratio between the particle and the matrix, $E_p/E_m$ with different values of the normalized particle's yield strength, $Y_p/E_m$ for the composite systems of a soft particle and a stiff matrix, i.e., $E_p/E_m < 1$.

The datum points presented in Fig. 6 show the numerical relationship between $h_p/R$ and the two variables, $E_p/E_m$ and $Y_p/E_m$, for the composite systems of a soft particle and a stiff matrix. Although it is very challenging, if not impossible, to determine the explicit scaling relationship of Eq. (8), curve fitting can be applied to find the functions, which best fit the three set of datum points. Matlab was applied and it was found that 6th order polynomial functions can be used to fit the points very well. The curves from the fitting functions are presented in Fig. 6. Their expressions are listed below:

$$\frac{h_p}{R} = 22.4\left(\frac{E_p}{E_m}\right)^6 - 54.58\left(\frac{E_p}{E_m}\right)^5 + 52.94\left(\frac{E_p}{E_m}\right)^4 - 25.81\left(\frac{E_p}{E_m}\right)^3 + 6.731\left(\frac{E_p}{E_m}\right)^2 - 0.8763\left(\frac{E_p}{E_m}\right) + 0.08589 \tag{9}$$

with $R^2 = 0.99994$ for $E_p/E_m < 1$ and $Y_p/E_m = 0.003$

$$\frac{h_p}{R} = 14.2\left(\frac{E_p}{E_m}\right)^6 - 35.38\left(\frac{E_p}{E_m}\right)^5 + 35.58\left(\frac{E_p}{E_m}\right)^4 - 18.08\left(\frac{E_p}{E_m}\right)^3 + 4.959\left(\frac{E_p}{E_m}\right)^2 - 0.6667\left(\frac{E_p}{E_m}\right) + 0.08855 \tag{10}$$

with $R^2 = 0.99997$ for $E_p/E_m < 1$ and $Y_p/E_m = 0.01$

$$\frac{h_p}{R} = -23.15\left(\frac{E_p}{E_m}\right)^6 + 56.11\left(\frac{E_p}{E_m}\right)^5 - 51.39\left(\frac{E_p}{E_m}\right)^4 + 22.68\left(\frac{E_p}{E_m}\right)^3 - 4.859\left(\frac{E_p}{E_m}\right)^2 + 0.5342\left(\frac{E_p}{E_m}\right) + 0.03514 \tag{11}$$

with $R^2 = 0.999993$ for $E_p/E_m < 1$ and $Y_p/E_m = 0.05$.

Considering the second type of composite system of a stiff particle and a soft matrix, $E_p/E_m > 1$, Fig. 7 shows the numerical results with three different values of the normalized particle yield strength, $Y_p/E_m$. In contrast to the first type of composite system, the influence of the particle's yield strength on the particle-dominated indentation depth is quite small and can be neglected in some cases for different values of $E_p/E_m$. Now the particle-dominated depth $h_p/R$ decreases with the modulus ratio $E_p/E_m$. When the value of $E_p/E_m$ is decreasingly approaches 1 from 1.5, the composite approaches to a single phase material, and as discussed before, the value of $h_p/R$ increases rapidly. Rational functions can be applied to fit the three set of datum points, see Fig. 7. The three functions are listed below:

$$\frac{h_p}{R} = \frac{0.5125\left(\frac{E_p}{E_m}\right) - 0.2805}{\left(\frac{E_p}{E_m}\right)^3 + 6.92\left(\frac{E_p}{E_m}\right)^2 - 2.316\left(\frac{E_p}{E_m}\right) - 8.205} \tag{12}$$

with $R^2 = 0.99993$ for $E_p/E_m > 1$ and $Y_p/E_m = 0.003$.

$$\frac{h_p}{R} = \frac{0.5442}{\left(\frac{E_p}{E_m}\right)^3 - 7.287\left(\frac{E_p}{E_m}\right)^2 + 32.09\left(\frac{E_p}{E_m}\right) - 27.85} \tag{13}$$

with $R^2 = 0.9994$ for $E_p/E_m > 1$ and $Y_p/E_m = 0.014$.

$$\frac{h_p}{R} = \frac{0.03107\left(\frac{E_p}{E_m}\right)^2 - 0.05653\left(\frac{E_p}{E_m}\right) + 0.07144}{\left(\frac{E_p}{E_m}\right)^3 - 3.746\left(\frac{E_p}{E_m}\right)^2 + 6.583\left(\frac{E_p}{E_m}\right) - 4.166} \tag{14}$$

with $R^2 = 0.9999994$ for $E_p/E_m > 1$ and $Y_p/E_m = 0.05$.

Author's personal copy



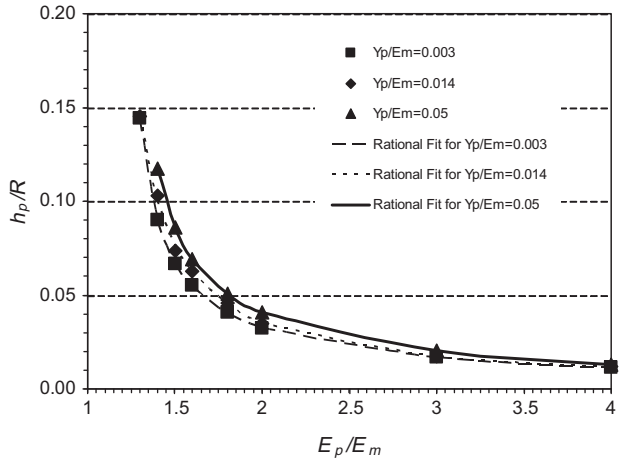


**Fig. 7.** The particle-dominated indentation depth, $h_p/R$, as a function of the elastic modulus ratio between the particle and the matrix, $E_p/E_m$ with different values of the normalized particle's yield strength, $Y_p/E_m$ for the composite systems of a soft particle and a stiff matrix, i.e., $E_p/E_m > 1$.

In terms of the potential application of the results in Fig. 7, $E_p/E_m > 1$ can be confirmed from the measured modulus versus indentation depth curve, which corresponds to a going-down curve with the increasing of the depth, see Fig. 5. The approach of trial and error, combined with the results presented in Fig. 7, can be used in practice to appropriately determine the elastic modulus of the particle. For example, if the measured elastic modulus of the particle normalized by the elastic modulus of the matrix is around 3, the indentation depth to obtain this modulus should be less than 1.3% of the particle's radius, otherwise, the error could be more than 10% according to Fig. 7. In another case, if the measured $E_p/E_m$ is around 1.5 and the indentation depth satisfies $h_p/R < 5\%$, then the measured result is also acceptable. The findings from this research are based on an idealized sharp indenter and an idealized flat specimen surface. To apply our finding directly in practice, these conditions should be satisfied as closely as possible. To quantify the influences from the roundness of the indenter tip and the surface roughness, further research is required.

## 4. Conclusion

Virtual indentation tests through computational finite element simulations were carried out to investigate the application of the Oliver–Pharr method to measure the elastic modulus of a particle embedded in a matrix. Due to indentation deformation of pile-up, the contact area should be measured directly from an indentation test and then used to predict the elastic modulus of the particle. The influence of the matrix on the measured result can be taken into account by bearing in mind the concept of a particle-dominated indentation depth. If the indentation depth is smaller than the particle-dominated indentation depth, the influence of the matrix can be neglected, i.e., the accuracy of the measure the particle's elastic modulus can be more than 90%.

Our parametric study indicates that the particle-dominated indentation depth strongly depends on the ratio of the particle's modulus to the matrix's modulus. If the ratio is smaller than one, the particle-dominated indentation depth increases with the modulus ratio. Additionally, the yield strength of the particle can affect the particle-dominated indentation depth. It increases with the increase of the particle's yield strength. If the ratio is greater than one, corresponding to the composites of a stiff particle embedded in a softer matrix, the particle-dominated indentation depth decreases with the modulus ratio. In these cases, the influence of the yield strength of the particle on the particle-dominated indentation depth can be neglected.

From the application point of view, whether the elastic modulus is smaller than that of the matrix or not can be determined by the trend of the measured indentation modulus versus the indentation depth curve. If the measured indentation modulus increases with the indentation depth, the ratio of the particle's modulus to the matrix's modulus is less than one. If the curve has the opposite trend, then the modulus ratio is greater than one. If the ratio is smaller than one, considering the value of the particle's yield strength is unknown, our numerical results suggest that the indentation depth should be no more than 5% of the particle radius. If the modulus ratio is larger than one, the permissible indentation depth predominantly depends strongly on the modulus ratio. Our numerical results presented in Fig. 7 or the fitting functions Eqs. (12)–(14) can be used to guide the indentation test.

## Acknowledgements

This research was undertaken at the NCI National Facility in Canberra, Australia, which is supported by the Australian Commonwealth Government. The authors are grateful to the two unknown reviewers for their helpful comments for improving the manuscript.

## References

[1] Cheng Y-T, Cheng C-M. Relationships between initial unloading slope, contact depth, and mechanical properties for spherical indentation in linear viscoelastic solids. Mater Sci Eng A 2005;409:93.
[2] Yan W, Sun Q, Feng X-Q, Qian L. Determination of transformation stresses of shape memory alloy thin films: a method based on spherical indentation. Appl Phys Lett 2006;88:241912.
[3] Yan W, Sun Q, Liu H-Y. Spherical indentation hardness of shape memory alloys. Mater Sci Eng A 2006;425:278.
[4] He LH, Fujisawa N, Swain MV. Elastic modulus and stress–strain response of human enamel by nanoindentation. Biomaterials 2006;27:4388.
[5] Fischer-Cripps AC. Critical review of analysis and interpretation of nanoindentation test data. Surf Coat Technol 2006;200:4153.
[6] Yan W, Pun CL. Spherical indentation of metallic foams. Mater Sci Eng A 2010;527:3166.
[7] Cao Y-P, Ji X-Y, Feng X-Q. Geometry independence of the normalized relaxation functions of viscoelastic materials in indentation. Phil Mag 2010;90:1639.
[8] Leggoe JW. Determination of the elastic modulus of microscale ceramic particles via nanoindentation. J Mater Res 2004;19:2437.
[9] Lee YH, Park JS, Higo Y, Kwon D. Nanomechanical properties of embedded dendrite phase and its influence on inelastic deformation of $Zr_{55}Al_{10}Ni_5Cu_{30}$ glassy alloy. Mater Sci Eng A 2007;449–451:945.
[10] Pradhan SK, Nayak BB, Sahay SS, Mishra BK. Mechanical properties of graphite flakes and spherulites measured by nanoindentation. Carbon 2009;47:2290.
[11] Delincé M, Jacques PJ, Pardoen T. Separation of size-dependent strengthening contributions in fine-grained Dual Phase steels by nanoindentation. Acta Mater. 2006;54:3395.
[12] Oliver WC, Pharr PM. An improved technique for determining hardness and elastic modulus using load and displacement sensing indentation experiments. J Mater Res 1992;7:1564.
[13] Bolshakov A, Pharr PM. Influences of pile-up on the measurement of mechanical properties by load and depth sensing indentation techniques. J Mater Res 1998;13:1049.
[14] Yan W, Pun CL, Wu Z, Simon GP. Some issues on nanoindentation method to measure the elastic modulus of particles in composites. Compos: Part B – Eng 2011;42:2093.
[15] Hay JL, Pharr PM. Instrumented indentation testing. ASM Handbook, vol. 8. Materials Park, OH: ASM International; 2000. p. 232–43.
[16] Sneddon IN. The relation between load and penetration in the axisymmetric Boussinesq problem for a punch of arbitrary profile. Int. J. Eng Sci. 1965;3:47.
[17] Oliver WC, Pharr GM. Measurement of hardness and elastic modulus by instrumented indentation: advances in understanding and refinements to methodology. J Mater Res 2004;19:3.
[18] Cheng Y-T, Cheng C-M. Scaling relationships in conical indentation of elastic–perfectly plastic solids. Int J Solids Struct 1999;36:1231.